8.5 Hail reflectivity signatures from two adjacent WSR-88Ds: carrier frequency and calibration issues

Valery Melnikov[*], Robert R. Lee[+], and Nicholas J. Langlieb[+]

[*]*Oklahoma University, CIMMS, and National Severe Storms Laboratory, Norman, OK.*
[+]*National Weather Service, Radar Operation Center, Norman, OK.*

1. Introduction

National Weather Service (NWS) operates a network of about 160 Weather Surveillance Radars WSR-88D, where D stands for Doppler and the numbers indicate the year of production. A frequency band from 2700 to 3000 MHz has been assigned for the radar carrier frequencies (S-band) corresponding to the wavelengths from 10 to 11.1 cm. Carrier frequencies of adjacent WSR-88D radars are offset to reduce signal interference. Changes in carrier frequencies slightly change radar parameters such as the antenna beamwidth, waveguide losses, and receiver sensitivity. An automatic calibration procedure, running on all radars, brings reflectivity values to the same level with accuracy of 1 dB.

The radar calibration procedure is based on basic engineering principles and assumes same scattering properties of weather echoes. One of the missions of the WSR-88Ds is precipitation measurement. The maximal stable size of raindrops is 6 mm which is small compared to the wavelength, i.e., 10 cm, so that the Rayleigh approximation for scattering properties are often used for rain. Sizes of hailstones can be a few centimeters and the Rayleigh approximation cannot be used in calculation of their scattering properties. For spherical hailstones, Mie theory is used. It follows from the theory that the radar cross section is an oscillating function of the diameter and wavelength so that radar backscattering cross sections and correspondingly reflectivities are different at different wavelengths. This is frequently called the resonant effect highlighting strong oscillations of scattering cross sections as functions of size or wavelength. This effect is used for hail detection with a two-wavelength radar, 3- and 10-cm, i.e., at X- and S-bands (Atlas and Ludlum 1961, Eccles and Atlas 1971, Doviak and Zrnic 2006, section 8.5.1) and at C- and S-bands (Féral et al. 2003), i.e., at highly diverse frequencies.

For radars at a narrow frequency band, it is assumed that small deviations of carrier frequencies do not change radar cross section substantially so that reflectivities are the same for the band. We analyze this assumption for rain and hail for the WSR-88D's frequency band and show that the resonant effect can cause a noticeable difference in reflectivity, Z, measured with adjacent WSR-88Ds. This means that adjacent radars, that use slightly different carrier frequencies, will measure different reflectivity values due to the resonant effect if hail is present.

The NWS is planning to upgrade the WSR-88D network with polarimetric capabilities in the near future (e.g., Istok, et al. 2009). The first prototype of the polarimetric WSR-88D is scheduled for deployment in 2010. Differential reflectivity, Z_{DR}, is one parameter measured by polarimetric WSR-88Ds. We also analyze the possible influences of the resonant effect on Z_{DR} at different carrier frequencies.

Sometimes clear air returns are used to compare calibrations on adjacent WSR-88D. Clear air echoes originate from turbulent fluctuations of refractivity as well as from flying birds and insects. The sizes of insects and birds can be sufficient to experience resonant scattering. In section 5 we show that reflectivities from two WSR-88Ds with different carrier frequencies can differ by several dB so that the verification of calibrations using clear air returns can be erroneous.

2. Radar data

Data from WSR-88D radars, KOUN and KCRI located in Norman OK, have been analyzed. The two radars are separated by about 243 m and operate at slightly different frequencies: 2705 MHz (KOUN) and 2995 MHz (KCRI). A severe thunderstorm containing hail was observed with the two radars on 5 November, 2008. KOUN collected data using VCP 32 and its tower is approximately 20 meters high. KCRI collected data in VCP 121 and its tower is approximately 30 meters high.

In Fig. 1, an example of PPIs from the two radars is presented. It is seen from the figure that areas with very strong reflectivity values, light magenta and white colors, are larger on KOUN than on KCRI. This difference could be a manifestation of resonant scattering effects in hail cores. When analyzing Z differences at the thunderstorm cores we have to be sure that Z calibrations on the radars are correct.

To be certain of the presence of the resonant effects we have to analyze the echoes on possible difference in radar calibration. We divided radar reflectivities, into three categories: 1) $Z < 20$ dBZ, 2) $20 \leq Z \leq 53$ dBZ, and 3) $Z > 53$ dBZ. The first category corresponds to clouds and light rain; the number of bins within this category depends on radar sensitivity. Hardware differences between WSR-88Ds lead to a difference in radar sensitivity which shows up as slightly different echo areas with $Z < 20$ dBZ. Fig. 2(a) presents time series of such areas observed with KOUN and KCRI. It is seen that KOUN is less sensitive than KCRI.

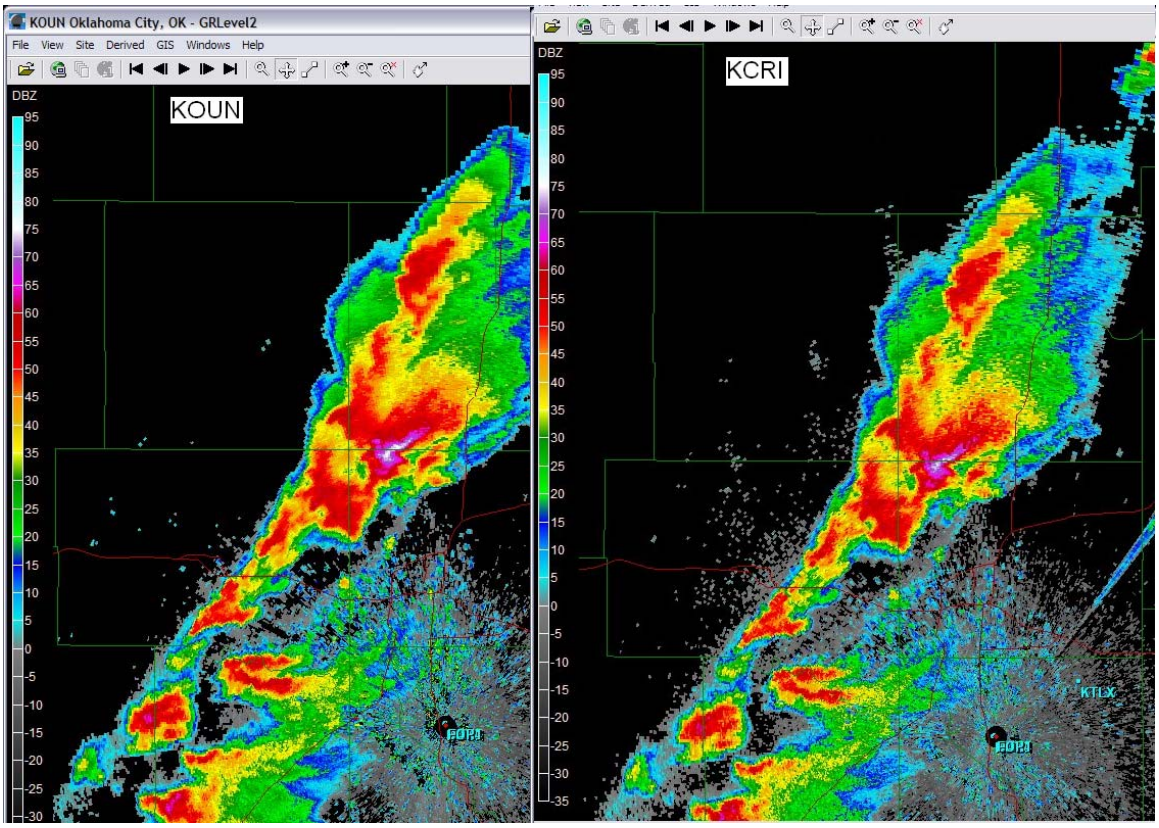

Fig.1. Reflectivity fields from (left) KOUN and (right) KCRI 5 November, 2008 at 21:45:25 (KOUN) and 21:46:01 (KCRI), elevations are 0.5^{o}.

The second Z category, i.e., $20 \leq Z \leq 53$ dBZ, corresponds to rain. Areas with these Z values should be equal on both radars because in rain, the calibration procedure brings radar reflectivity to same level. One can see from Fig. 2(b) that areas of Z of second category are equal. This means Z calibrations on the radar are close.

The third Z category, i.e., $Z > 53$ dBZ corresponds to possible presence of hail. WSR-88D precipitation algorithms use 53 dBZ, in effect, to delineate rain from hail (Fulton et. al. 1998). Therefore, in areas with $Z > 53$ dBZ, hail is likely. Fig. 2(c) shows that starting at 21:15 Z, KOUN detects more reflectivity bins within the third category than KCRI. For very high Z values ($Z > 60$ dBZ), one can see the same tendency: KOUN detects more bins, a larger area, than KCRI most of the time (Fig 2(d)). Thus we conclude that KOUN frequently has higher reflectivity values and a larger area with high Z values than KCRI does on this day.

A discrepancy in reflectivity values measured with two radars can be due to differences in many parameters: heights of radar towers, nonlinearities of the receivers, antenna elevation angles, clutter maps, VCPs used, time lag between observations with two radars. The antennas of KOUN and KCRI are at 20 and 30 m, respectively, above the ground and the radars are located 243 m apart. These differences cause small displacement of the radar resolution volumes. Because of different antenna heights the radar clutter maps are not similar for the radars. We analyzed data wherein the vast majority of the echoes were beyond the range with strong ground clutter contamination and we believe that this did not influence our results significantly.

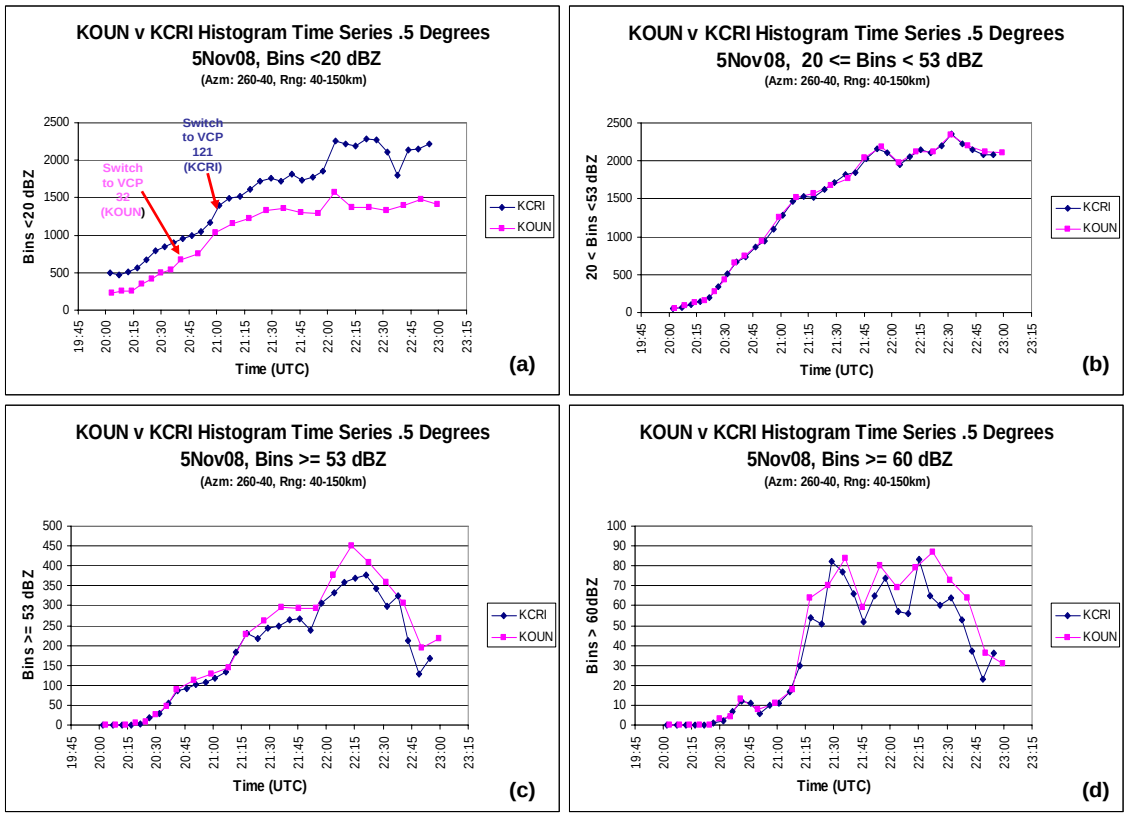

Fig. 2. Time series comparisons of areas with given reflectivities collected with KOUN (the magenta line) and KCRI (the blue line) for reflectivities in intervals (a) less than 20 dBZ, (b) between 20 and 53 dBZ, (c) larger than 53 dBZ, and (d) larger than 60 dBZ.

Nonlinearity of the new ORDA receivers should be less than 0.5 dB and we believe could not lead to noticeable reflectivity differences. Different VCPs should not cause Z value differences as far as the calibration procedure makes radar reflectivity equal in rain; however, VCP 121 averages 17 radar pulses per sample volume while VCP 32 averages 64 pulses per sample volume. Differences in elevation angles lead to different heights of the radar volumes. We analyzed data from the lowest elevation, i.e., 0.5^{o}, and noticed that the elevation difference was approximately 0.1^{o} which translates to height difference of 52 m at 30 km. In hail cores of thunderstorms, reflectivity gradients can be strong so that the difference in radar volume heights can cause discrepancies in measured reflectivities. Another uncertainty comes from time lag between sweeps from the two radars. The latter two uncertainties do not allow linking measured reflectivity differences to the resonant effect entirely. So despite measured reflectivity differences we cannot conclude that this is due to scattering effects. Additional experimental evidence is needed. But the strong tendency of KOUN to observe higher Z values than KCRI points to scattering differences at different wavelengths. In the next section we analyze an influence of resonant scattering effects on observed difference of high reflectivity values.

3. Results of calculations

The power P of received radar signal is proportional to the backscatter cross section σ_b (Doviak and Zrnic, 2006, section 4.4)

$$P_\lambda = (C_\lambda P_t / r^2) \sum \sigma_{bi} ,$$

where P_t, C_λ, and r are the transmitted power, radar constant, and range to the radar volume; the summation contains all scatterers in the radar volume. The received power is proportional to measured reflectivity factor Z. The ratio of received powers measured with two radars with two different wavelengths λ_1 and λ_2 is

$$\frac{P_{\lambda 1}}{P_{\lambda 2}} = \frac{C_{\lambda 1} P_{t1} \sum \sigma_{bi}(\lambda_1)}{C_{\lambda 2} P_{t2} \sum \sigma_{bi}(\lambda_2)} =$$

$$\frac{C_{\lambda 1} P_{t1} \int \sigma(D, \lambda_1) N(D) dD}{C_{\lambda 2} P_{t2} \int \sigma(D, \lambda_2) N(D) dD}$$

where $N(D)$ is the size distribution, i.e., the number of particles with diameter D. The radar calibration procedure brings the radar constants to such levels that for small particles (e.g., raindrops) $P_{\lambda 1} = P_{\lambda 2}$. For large particles (e.g., hailstones) this equality does not hold. Due to a strong dependence of the cross sections on wavelength, i.e., due to the resonant effect, reflectivity values from two radars can differ. This difference depends on the wavelengths and sizes of hydrometeors (rain or hail). To calculate radar reflectivity for hailstones, we utilized the T-matrix method (Mischenko et al. 2002). Since reflectivity Z is proportional to the logarithm of received powers then the difference of measured reflectivity values at two wavelengths is

$$Z_{\lambda 1} - Z_{\lambda 2} = 10 \log[\int \sigma(D, \lambda_1) N(D) dD / \int \sigma(D, \lambda_1) N(D) dD], \quad (dB) \qquad (1)$$

Large raindrops are very oblate and we approximate their shapes with oblate spheroids with semi-axes proposed by Brandes et al. (2002). The drop size distribution was used according to Marshall and Palmer (e.g., Doviak and Zrnic, 2006, section 8.1.2):

$$N(D) = N_o \exp(-\Lambda D), \qquad (2)$$

$$\Lambda = 4.1 R^{-0.21},$$

$$N_o = 8\ 10^3\ m^{-3} mm^{-1}$$

where R is the rain rate in mm per hour, and D is the diameter of drop in mm. Calculations via (1) show that for rain rates up to 150 mm h^{-1}, the reflectivity value difference at the two wavelengths remains less than 0.1 dB, thus this difference can be neglected.

If hail is present in the radar volume, the difference of radar cross sections can reach several dB. In Fig. 3(a), this difference is shown for spherical hailstones as a function of the diameter. Hailstones can be dry, wet, or spongy. Dry hailstones do not contain water on their surface and inside. If there is a water film on the surface of a hailstone, such hailstones are usually called wet. Spongy hailstones consist of a mixture of ice and water. In Fig. 3(a), the ratios of radar cross sections for two wavelengths are depicted for different thickness of water films on their surfaces. The thickness 0 mm (the blue line in the figure) corresponds to dry hailstones. One can see that water films make resonant effects more pronounced and shift the first resonant peak toward smaller sizes. The difference in scattered powers can easily exceed 5 dB and can reach 20 dB for water films about 0.1 mm. The difference exceeds 2 dB at diameters about 3 cm and is positive for smaller hailstones and becomes negative for large ones.

Size distributions $N(D)$ of hailstones can be of different shapes. Smaller sizes have been represented by an exponential function like in (2) or a gamma function (Cheng and English 1983, Federer and Wladvogel 1975) but large sizes often seem to have narrow distributions centered on the mean (Ziegler et al. 1983). Thus we consider different $N(D)$. Results for a uniform distribution between *Dmin* and *Dmax* with *Dmax* - *Dmin* = 1 cm are presented in Fig. 3(b) as a function of *Dmax*. It is seen that the reflectivity difference can exceed 2 dB for hailstones with diameters larger than 3.5 cm and reaches 6 dB at *Dmax* = 4.5 cm for wet hailstones. For uniform and exponential distributions, shown in Figs. 3 (c,d), the Z difference can be 2 dB for *Dmax* in the interval 3.5 to 5 cm. In our calculations, we used Λ=0.3 (Doviak and Zrnic 2006, section 8.1.3).

Two general conclusions that can be deduced from Fig. 3 are as follows. 1) Resonant effects can produce a reflectivity difference at close wavelengths as high as 6 dB and higher than 2 dB in a large interval of hailstones diameters from 3.5 to 5 cm. 2) The reflectivity difference can be positive and negative; it is mainly positive for hailstones with diameters smaller than 4.5 cm and it is mainly negative for larger diameters. From these conclusions we deduce that if the hailstone

diameter is smaller than 4.5 cm, KOUN reflectivity values can exceed reflectivity values from KCRI, which corresponds to radar data presented in the previous section (Figs. 2(c, d)). For larger hailstones, a vice versa correspondence can take place, i.e., KCRI's reflectivity values can be larger than KOUN's reflectivity values.

We conclude that estimations of radar "hotness" by comparing radar echoes from two adjacent WSR-88D should be done in precipitation areas corresponding to rain, i.e., at reflectivity values less than 53 dBZ. Radar reflectivity values in cores of thunderstorms can be different due to the resonant effect rather than calibration differences.

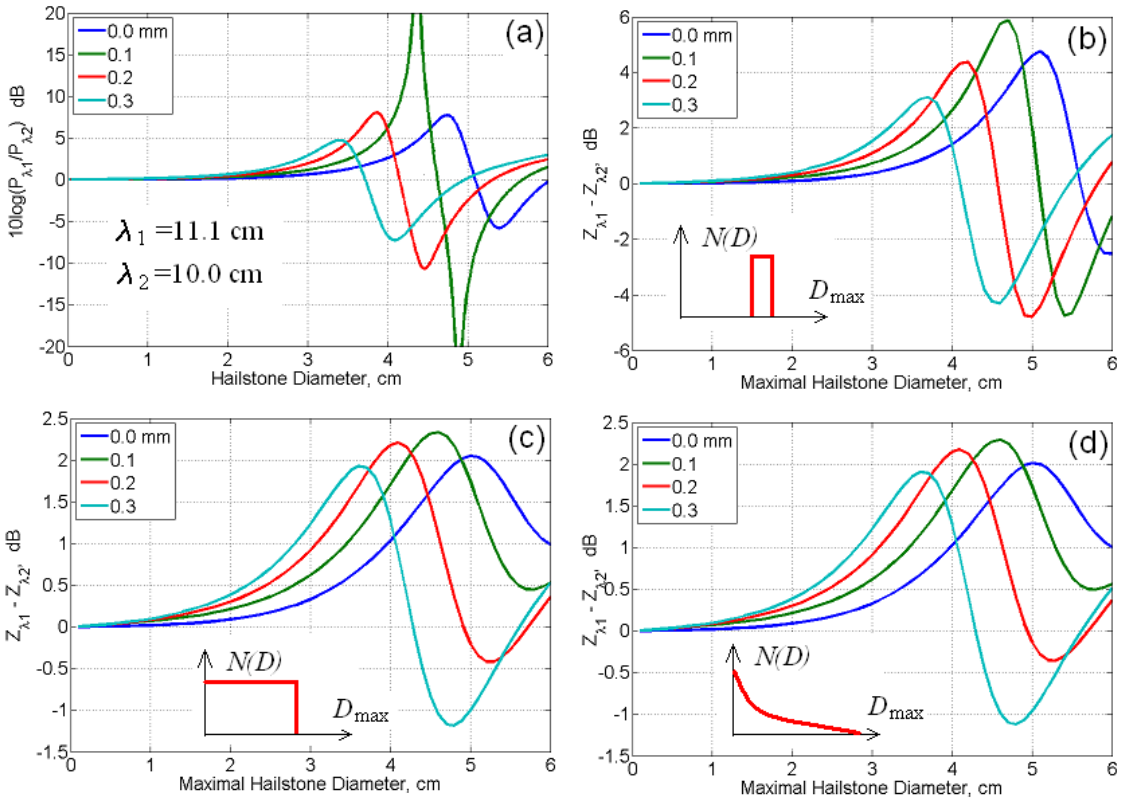

Fig. 3. (a): The difference of backscatter cross sections of hailstones at two wavelengths corresponding to KOUN (λ=11.1 cm) and KCRI (λ=10.0 cm). (b) – (d): reflectivity differences measured at the two wavelengths for three forms of size distributions shown in the inserts. The thickness of water films on hailstones is indicated in the legends.

4. Differential reflectivity

The NWS is planning to upgrade the WSR-88D network with polarimetric capabilities in the near future (e.g., Istok, et al. 2009). The first prototype of the polarimetric WSR-88D is scheduled for deployment in 2010. The proof-of-concept WSR-88D KOUN employs a polarimetric mode with simultaneous transmission and reception of horizontally and vertically polarized waves (Zrnic et al., 2006).

Simultaneously with the base radar variables, polarimetric WSR-88Ds will routinely measure the following polarimetric variables: 1) differential reflectivity, Z_{DR}, 2) total differential phase, ϕ_{DP}, and 3) the copolar correlation coefficient ρ_{hv} (e.g., Doviak and Zrnic, 2006, section 6.8). It was demonstrated in the previous section that slight difference in the carrier frequency can lead to noticeable difference in reflectivity values due to the resonant effect. In this section we analyze an impact of this effect on differential reflectivity.

Radar observations show that hail can have positive and negative Z_{DR}. Usually positive

Z_{DR}, is associated with oblate hailstones falling with the major axis being about horizontal. Negative Z_{DR} is usually associated with conical hailstones falling with the major axis being vertical. Resonant effects make this consideration more complicated: nonspherical scatterers experience different resonances at different dimensions. In Fig. 4(a) for oblate ice spheroid, one can see that oblate scatterers produce negative Z_{DR} for diameters larger than about 50 mm. A similar feature exhibits prolate hailstones (Fig. 4c). This is in contrast to rain wherein oblate raindrops produce positive Z_{DR} only. The difference of Z_{DR}, measured at two wavelengths remains close to zero for prolate and oblate hailstones with sizes less than 5 cm. Thus differences in Z_{DR} measured from two WSR-88Ds point to the presence of very large hailstones with diameters larger than 5 cm.

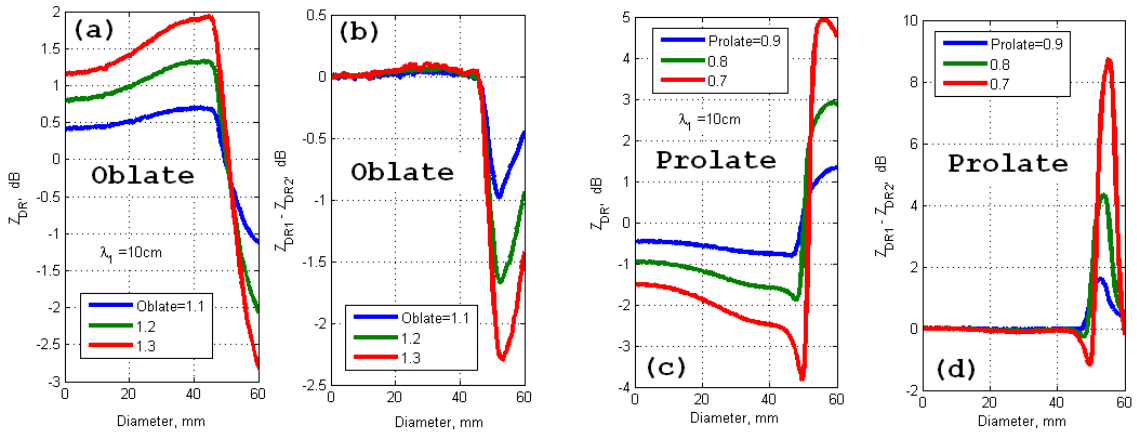

Fig. 4. (a): Differential reflectivity of oblate ice spheroids with oblateness 1.1, 1.2, and 1.3 and (b) the difference of Z_{DR} at two wavelengths corresponding to KOUN (λ=11.1 cm) and KCRI (λ=10.0 cm). (c) and (d) same as in (a) and (b) but for prolate spheroids.

5. Effects in clear air

Resonant effect can manifest itself in clear air radar observations. In clear air conditions, radar echo is formed by turbulent fluctuations of air, flying insects, and birds. Birds are not small species compared to S-band wavelength so that the resonant effects are significant for them (e.g., Zrnic and Ryzhkov 1998). Vaughn (1985) reported that width-to-length ratios for birds vary between 1:2 and 1:3, i.e., birds can be considered as quite prolate scatterers.

The two top panels in Fig. 5 present reflectivity fields from KOUN and KCRI collected on 13 May, 2009 at 0401Z. A large echo from migrating birds with reflectivities up to 30 dBZ extends to distances of 100 km. Echoes from thunderstorms with reflectivity values exceeding 50 dBZ stretch from north-west to south-west. The reflectivity difference from the two radars, ΔZ, is shown in panel (c) of Fig. 5. In areas with precipitation, ΔZ is patchy because of slight differences in antenna elevations and times of data collection. Precipitation areas with positive and negative ΔZ are about equal where the two radars measure similar reflectivity values. In bird echoes, reflectivity values from KOUN are larger than reflectivity values from KCRI: the difference reaches 16 dB. We attribute this difference to the resonance effect. Roughly, a bird body can be represented with a water sphere. In Fig 5(d), the difference of reflectivity values at two wavelengths is shown for water spheres as a function of their diameter. It is seen that the difference exceeds 10 dB for diameters 5.2 to 5.5 cm. So the reflectivity value difference measured from two adjacent WSR-88Ds can be used to estimate the diameter of bird species.

The length of large insects reaches 5.5 cm (Vaughn 1985, Wilson et al. 1994) which is more than half of the wavelength of the WSR-88Ds so that resonant effects can be significant in “clear air” observations. According to Vaughn (1985), width-to-length ratios for insects vary between 1:3 and 1:10, i.e., insects are strongly prolate scatterers. We assume that the dielectric constants for insects and birds are equal to that of water. T-matrix code available can handle prolate spheroids with width-to-length ratios smaller than 1:3 which is the largest ratio for birds but is the smallest ratio for insects.

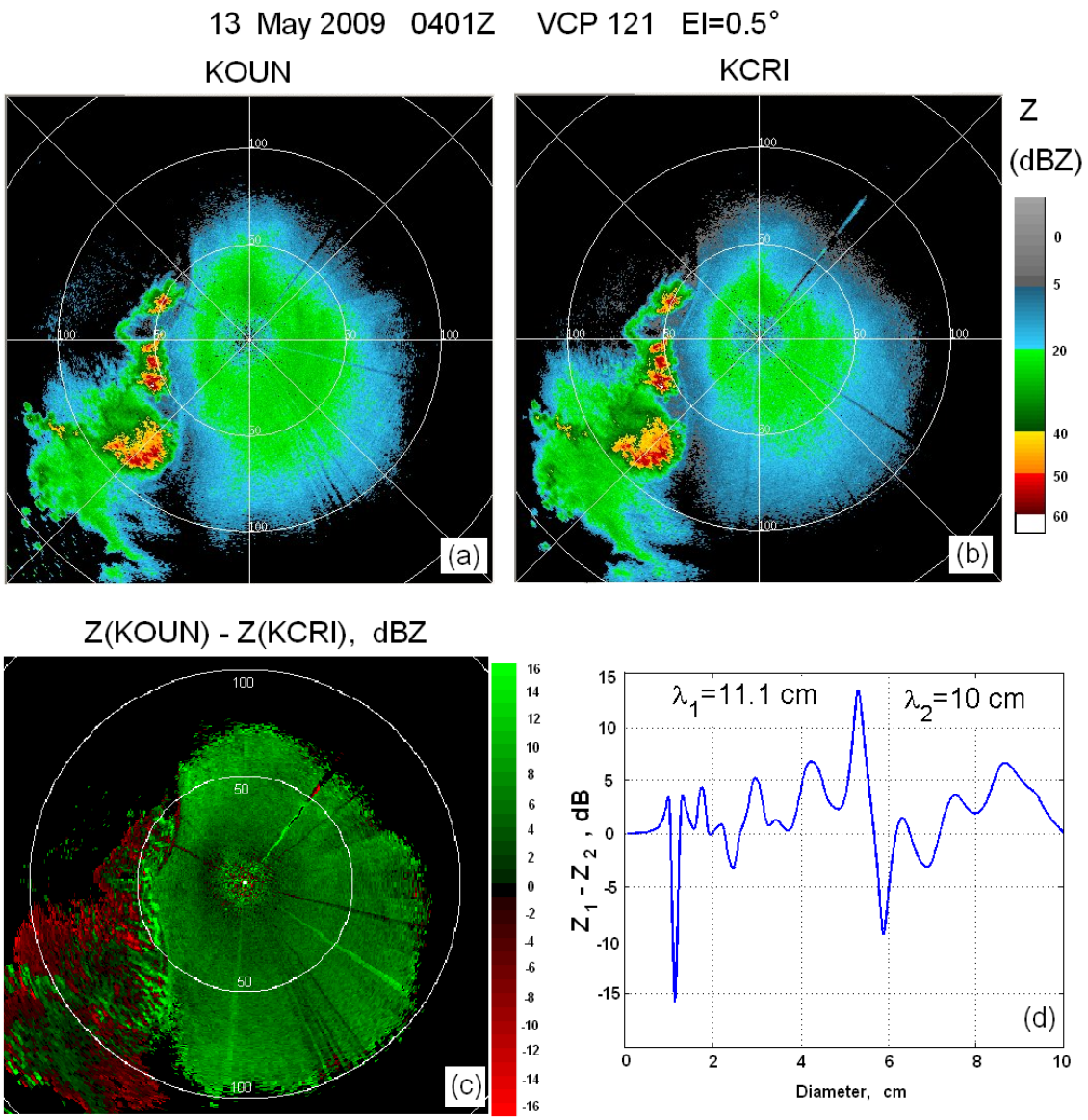

Fig. 5. (a, b): Reflectivity from KOUN and KCRI on 13 May, 2009 and (c) reflectivity difference (d): reflectivity difference at two wavelengths for water spheres.

The reflectivity difference at two wavelengths corresponding to KOUN and KCRI radars is shown in Fig. 6(a) for prolate spheroids at temperature 20°C. It is seen that for scatterers with lengths around 1.2 cm, KCRI's reflectivity is larger than KOUN's reflectivity. For scatterers with sizes larger than 3 cm, KOUN's reflectivity can exceed KCRI's reflectivity. That is in the presence of insects in the radar volume, reflectivity values can differ significantly. Consequently, estimates of "hotness" between two adjacent WSR-88Ds by using "clear air" echoes can be erroneous due to resonant scattering effects.

Clear air returns cannot be used in comparisons of differential reflectivities measured with adjacent WSR-88Ds. Fig. 6(b) presents calculated differences in Z_{DR} for KOUN and KCRI for prolate spheroids with different aspect ratios. It is seen that the difference reaches 6 dB for species of 1 to 2 cm long with aspect ratios 1:3. The difference increases with increasing aspect ratio. So we conclude that "clear air" echoes should not be used to compare radar calibrations between adjacent WSR-88Ds with different carrier frequencies.

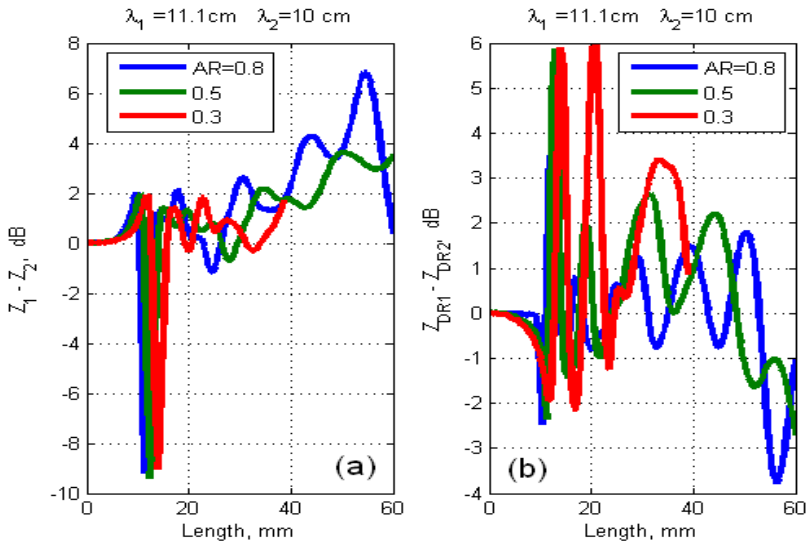

Fig. 6. (a): The difference of reflectivities at two wavelengths corresponding to KOUN (λ=11.1 cm) and KCRI (λ=10.0 cm) for prolate spheroids (b): The difference of differential reflectivities at the same wavelengths. Width-to-length ratios (i.e., aspect ratios, AR) are indicated in the legends.

Conclusions

To reduce signal interference among adjacent WSR-88Ds, carrier radar frequencies are offset. Shifts in carrier frequency slightly alter the antenna beamwidth, signal losses in the waveguides, and receiver sensitivity. The calibration procedure running on the WSR-88Ds adjusts the radar constant and makes reflectivities equal. This implies that scattering media remains the same for different carrier frequencies. We analyzed this assumption for rain and hail and showed that in the presence of hail, reflectivities from adjacent WSR-88Ds can differ due to resonant scattering effects for hailstones. Calculations show that the reflectivity difference can reach 6 dB and depends on sizes of hailstones, their wetness, and the shift in radar carrier frequencies. For hailstones with sizes less than 4 cm, reflectivity from KOUN should exceed reflectivity from KCRI.

We analyzed a hail case observed on 5 November, 2008 with WSR-88D KOUN with the wavelength of 11.1 cm and KCRI with the wavelength of 10.0 cm. The distance between the radars is 243 m, i.e., they are practically collocated. Radar observations show that echoes with reflectivity values between 20 and 53 dBz were equal on the day. This reflectivity interval corresponds to rain. Equality of areas with these reflectivities points to good calibration of the radars (Fig. 2b).

Reflectivity of 53 dBZ is used on the WSR-88D network as a threshold indicating hail presence. Areas with radar echoes with reflectivities larger than 53 dBZ are larger on KOUN than on KCRI (Fig. 2c). This is in accord with theoretical predictions drawn from the resonant effect. So estimation of calibration correctness, i.e., "hotness" of radars should be done in areas with reflectivities between 20 and 53 dBZ wherein resonant effects are absent. Reflectivity values in thunderstorm cores measured with adjacent WSR-88Ds can be different, caused by the resonant effect, if hail is present. A slight difference in elevation angles and a time lag between radar sweeps on KOUN and KCRI do not allow us to attribute measured reflectivity differences entirely to the resonant scattering effect. We consider the observed difference as an indication of the resonance. More radar observations are needed to be more confident.

The NWS is planning on upgrading the WSR-88D to polarimetric capabilities so that differential reflectivity will be one of the new measureable radar parameters. Our calculations show that differential reflectivity values measured from adjacent WSR-88Ds are equal in rain and hail if the maximal hailstone diameter is smaller than 5 cm. For larger diameters, differential reflectivities can be different due to the resonant effect.

The resonant effect can also manifest itself in radar echoes from "clear air", i.e., in scattering by birds and insects. Reflectivity values measured with KOUN and KCRI can differ by more than 10 dB (Fig. 5c). So estimation of "hotness" of a radar using clear air returns can be erroneous. Differential reflectivities from KOUN and KCRI in "clear air" can also differ significantly due to the resonant effect in scattering from birds and large insects.

References

Atlas, D., and F. H. Ludlum, 1961: Multi-wavelength radar reflectivity of hailstorms. *Quart. J. Roy. Meteor. Soc.,* **87,** 523–534.

Battan, L. J., 1973: *Radar observation of the atmosphere*. University of Chicago, 324 pp.

Brandes, E.A., G. Zhang, and J. Vivekanan-dan, 2002: Experiments in rainfall estimation with a polarimetric radar in a subtropical environment. *J. Appl. Meteor*., **41**, 674 – 685.

Cheng, L., and M. English, 1983: A relation- ship between hailstone concentration and size. *J. Atmos. Sci.* **40,** 204-213.

Doviak, R. J. and D. S. Zrnic, 2006: *Doppler radar and weather observations*, 2nded., Dover Publications, 562 pp.

Eccles, P. J., and D. Atlas, 1973: A dual-wavelength radar hail detector. *J. Appl. Meteor.,***12,** 847–854.

Fulton, R. A., J. P. Breidenbach, D-J. Seo, D. A. Miller, and T. O'Bannon, 1998: The WSR-88D Rainfall Algorithm. *Wea. Forecasting,* **13**, 377 - 395.

Federer, B., and Wladvogel, 1975: Hail and raindrop size distributions form a Swiss multicell storm. *J. Appl. Meteor.,* **14,** 91-97.

Féral, L., H. Sauvageot, and S. Soula, 2003: Hail detection using S and C-band radar reflectivity difference. *J. Atmos.Oceanic Technol.,* **20,** 233–248.

Istok, M., M. Fresch, Z. Jing, S. Smith, R. Murnan, A. Ryzhkov, J. Krause, M. Jain, P. Schlatter, J. Ferree, B. Klein, D. Stein, G. Cate, R. Saffle, 2009: WSR-88D dual-polarization initial operational capabilities. *25*th *Conf. on IIPS, Amer. Meteorol. Soc*., Phoenix, AZ, 15.6.

Lang, T.J., S.A. Rutledge, and J.L. Smith, 2004: Observations of quasi-symmetric echo patterns in clear air with the CSU-CHILL polarimetric radar. *J. Atmos. Oceanic Technol.,* **21**, 1182-1189.

Meneghini, R., and T. Kozu, 1990: *Spaceborn Weather Radar*. Boston, MA, Artech House.

Meneghini, R., and L. Liao, 1996: Comparison of cross sections for melting hydrometeors as derived from dielectric mixing formulas and a numerical method. *J. Applied Meteor*., **35**, 1658-1670.

Mischenko M. I., L.D. Travis, and A.A. Lacis, 2002: *Scattering, Absorbtion, and Emission of Light by Small Particles.* Cambridge University Press, 228 pp.

Muller, E.G., and R.P. Larkin, 1985: Insects observed using dual-polarization radar, *J. Atmos. Oceanic Technol*., **2**, 49-54.

Vaughn, C. R. 1985: Birds and insects as radar targets. A review. *Proc. IEEE*, **73**, 205- 227.

Wilson, J.W., T.M. Weckwerth, J. Vivekanandan, R.M.Wakimoto, and R.W. Russel, 1994: Boundary layer clear-airradar echoes: Origin of echoes and accuracy of deriving winds. *J. Atmos. Oceanic Technol*., **11**, 1184-1206.

Witt, A., M. D. Eilts, G. J. Stumpf, J. T. Johnson, E. D. Mitchell, and K. W. Thomas, 1998: An enhanced hail detection algorithm for the WSR-88D. *Wea. Forecasting,* **13,** 286–303.

Zeng, Z., S. E. Yuter, R. A. House, and D. E. Kingsmill, 2001: Microphysics of the rapid development of heavy convective precipitation. *Mon. Wea. Rev.,* **129,** 1882–1904.

Ziegler C.L., P.S. Ray, and N. C. Knight, 1983: Hail growth in an Oklahoma mutlicell storm. *J. Atmos. Sci.* **40,** 1768-1791.

Zrnic, D. S., and A.V. Ryzhkov, 1998. Observations of insects and birds with a polarimetric radar. *IEEE Trans. Geosci.Remote Sens*., **36**, 661-668.